RECONSIDER PHOTOPLETHYSMOGRAM SIGNAL QUALITY ASSESSMENT IN THE FREE LIVING ENVIRONMENT

YAN-WEI SU, CHIA-CHENG HAO, GI-REN LIU, YUAN-CHUNG SHEU, AND HAU-TIENG WU

Abstract. Background: Assessing signal quality is crucial for biomedical signal processing, yet a precise mathematical model for defining signal quality is often lacking, posing challenges for experts in labeling signal qualities. The situation is even worse in the free living environment. Method: We advocate a reconsideration of the concept of signal quality. Result: We demonstrate the necessity of this reconsideration and highlight the relationship between signal quality and signal decomposition with examples recorded from the free living environment. Conclusion: A new method, distinct from visually inspecting the raw PPG signal to assess its quality, is needed. Our proposed ANHM model, combined with advanced signal processing tools, shows potential for establishing a systematic signal decomposition based SQA model.

1. Introduction

Various methods exist for assessing the quality of a photoplethysmogram (PPG) signal [11]. Fundamental criteria, such as the presence of clear pulse peaks, are essential for basic signal quality [16], facilitating heart rate (HR) extraction through peak detection algorithms [4]. Diagnostic quality demands clean pulse waveforms, or cardiac components, with visible systolic and diastolic waves [12]. Additional considerations include pulse amplitude and width consistency with adjacent pulses, and adherence to typical PPG pulse morphology (primary and secondary peaks, troughs, pulse amplitude, width, etc.) [21]. Alternatively, simultaneous recording of other signals, as demonstrated in [14], can be employed to define quality by comparing PPG-derived HR to electrocardiogram (ECG)-derived HR. To our knowledge, generally, experts seem to rely on the visibility of the cardiac component to label the quality of a PPG segment. To automatically quantify PPG quality, signal processing techniques are needed. This can be achieved through time-domain, frequency-domain, or hybrid approaches, guided by predefined rules or machine learning techniques. See [16, 11] for a review of available tools.

Despite implicitly consented PPG signal quality criteria among experts and numerous proposed PPG signal quality assessments (SQA) algorithms, there is, to our knowledge, no paper precisely defining what PPG signal quality really means with a mathematical model, particularly in the context of subjects moving in a free-living environment. As a result, PPG signals with multiple components, especially involving moving rhythms with the movement rhythm close to HR, may be considered of low or high quality due to the presence of "non-cardiac" artifacts depending on the potential phase synchronization between heart rate and moving rhythm. See Figure 1 for an example of a "low quality" PPG and Figure 4 for a

"high quality" PPG, both are recorded during exercise, and experts' label. Consider that various sources of "non-cardiac" artifacts can significantly alter the PPG waveform, such as sudden breathing changes, body movements, or talking. In the pursuit of *extracting cardiac information* from the PPG component, it is crucial to minimize irrelevant factors like respiration and motion artifacts, especially in a free-living environment. Addressing these artifacts is a challenging task. Since the respiration is usually of much lower frequency, it usually can be suppressed by a high-pass filter. Several algorithms have been proposed to reduce motion artifacts [7, 18, 9, 13, 17] as a pre-processing stage for robust heart rate detection. We could view some of these motion artifact removal algorithms as a special case of the general signal decomposition mission. To our knowledge, the relationship between signal decomposition and signal quality has not been well studied.

Motivated by the critical role played by the signal quality in biomedical signal processing, we advocate the necessity of reconsidering what it means by the signal quality using PPG, and the necessity for a precise definition of signal quality based on a well defined mathematical model that is oriented by the scientific target. We emphasize the close connection between signal quality definition and the signal decomposition problem, particularly in handling non-sinusoidal oscillatory patterns of respiration and motion in the PPG signal, by modeling the PPG signal with the *adaptive non-harmonic model* (ANHM). For instance, respiration-induced intensity variation (RIIV) and motion rhythm, being non-sinusoidal when exists, may introduce spectral interference with the cardiac component. Armed with this signal decomposition technique, we provide a detailed exploration of potential issues of existing signal quality labeling approach that may arise without a precise signal quality definition.

2. Mathematical model and signal decomposition

To model a PPG signal, we indicate some observations. First, due to the heart rate variability, the frequency of the cardiac component is time-varying. Second, the respiration may impact the oscillatory strength of the cardiac component or exist as an additional oscillatory component called RIIV [19]. Motion rhythm might exist if a subject is moving. Third, the trends, or direct currents (DCs), of red and infrared channels encode the oxygen saturation information [8]. Fourth, noise is inevitable. Jointly, we consider the *adaptive non-harmonic model* (ANHM) [22] to model the PPG signal. Fix small constants $\epsilon > 0$ and $\Delta > 0$. A clean PPG is modeled by

$$f_0(t) = \sum_{\ell=1}^{L} a_\ell(t) s_\ell(\phi_\ell(t)) + T(t)\,, \tag{1}$$

where $a_\ell(t)s_\ell(\phi(t))$ is called the *intrinsic model type* (IMT) function fulfilling some conditions listed below and $T(\cdot)$ is a smooth function so that its Fourier transform $\hat{T}$ is compactly supported in $[-\Delta, \Delta]$. For each $\ell \in \{1, \dots, L\}$, we assume

- (C1) $\phi_\ell(t)$ is a C^2 function, which is called the *phase function* of the ℓ-th IMT function;
- (C2) $\phi'_\ell(t) > 0$, which is called the *instantaneous frequency (IF)* of the ℓ-th IMT function. We assume $|\phi''_\ell(t)| \le \epsilon\phi'_\ell(t)$ for all $t \in \mathbb{R}$;
- (C3) $a_\ell(t) > 0$ is a C^1 function, which is called the *amplitude modulation (AM)* of the ℓ-th IMT function so that $|a'_\ell(t)| \le \epsilon\phi'_\ell(t)$ for all $t \in \mathbb{R}$;

(C4) $s_\ell(\cdot)$ is a smooth 1-period function with mean 0 and unit L^2 norm so that $|\hat{s}_\ell(1)| > 0$, which is called the *wave-shape function* (WSF) of the ℓ-th IMT function;

(C5) when $L > 1$, we assume $\phi'_\ell(t) - \phi'_{\ell-1}(t) \geq d$ for $\ell = 2, \ldots, L$, where $d > 0$.

In practice, since we can easily remove the trend component T by applying a high-pass filter in the pre-processing step, from now on we assume $T = 0$ to simplify the discussion. A more complicated model could be considered [10], but to avoid distracting from the discussion of signal quality, we are satisfied with this ANHM model. See signals shown in Figures 1 and 4 for examples with $L = 2$. It is difficult to visualize the cardiac oscillatory pattern in the raw PPG signal. Thus, a tool that decomposes the signal into IMT components plays an important role when we want to analyze the oscillatory signal of the type (1).

For signal decomposition, we apply the recently developed algorithm Shape-Adaptive Mode Decomposition (SAMD) [1] to obtain each IMT function. In short, we estimate the IF of each IMT function with a preferred time-frequency (TF) analysis algorithm [5]. In this work we choose the second order synchrosqueezing transform (SST) [2, 15] with the recently developed ridge extraction algorithm, *multiple harmonics ridge detection* (MHRD) [20], to obtain a reliable ridge that represents the IF [3], and hence the phase and AM. SAMD is a nonlinear optimization algorithm that takes the estimated phase and AM of each IMT function to reconstruct each IMT function.

3. Reconsider what the signal quality should be

We shall now discuss a critical issue regarding what signal quality should be defined. We demonstrate the issue using signals from the publicly available dataset TROIKA [23] with experts' annotation from [6]. In the TROIKA dataset, both the PPG signal and triaxial acceleration signal were recorded from the wrist. Subjects performed treadmill running with changing speeds during data collection. The labels assign binary values (1 for "artifact" or "low quality", and 0 for "clean", "no artifact" or "high quality") to each sample point in the segment. The TROIKA dataset was pre-processed by its original author in [23] with bandpass from 0.4 Hz to 5 Hz.[1] To be consistent, we pre-process the databases used in [6] by applying a 6th-order Butterworth filter with a low end cutoff of 0.5 Hz and a high end cutoff of 20 Hz. All the 30-second PPG segments are uniformly sampled at the sampling rate of 64 Hz, and the signal values are normalized to the range $[0, 1]$. We delineate the label generation process [6]. Binary labels were established by annotators through assessing the correlation between ECG and PPG heartbeats, and examining the regularity of PPG signals to identify artifacts. Two scenarios were considered: (1) If motion is detected in the accelerometer and irregularities align with the accelerometer data, the segment is marked as an artifact. (2) If no motion is detected in the accelerometer, ECG displays normal sinus rhythm, but irregularities are present in the PPG signal, the segment is marked as an artifact. Each signal was annotated by at least one annotator. Initially, fifty 30-second segments were randomly selected and independently annotated by three annotators. Annotations were compared and analyzed, and decisions were made collectively to improve agreement. Subsequent annotations were conducted by a single annotator.

[1] See [6] and the description in [23]

See Figure 1 for an example PPG segment, the 65.5th second to the 76th second segment, from the 6th subject in the TROIKA database [23] (`DATA_06_TYPE02.mat`), when the subject is running at the speed of 6 kilometer per hour during this segment. The label sequence provided by experts [6] is depicted as the gray curve in the first row. Examining the raw signal in the second row may encourage labeling the segment to have low quality due to its chaotic oscillation pattern, and some subsegments are labeled "no artifact" (or high quality) based on visually identifiable "regular" oscillations mimicking cardiac patterns. However, is this label really what we want? To confirm if this label is authentic, we dig into the ground truth by inspecting the simultaneously recorded ECG signal (red curve in the fourth row) and accelerometer magnitude signal (red curve in the third row). To enhance the visualization, the R peak locations are superimposed on the second row as gray vertical lines. We find that the seemingly regular subsegments in PPG do not align with the cardiac oscillation. This raises concerns about determining signal quality from the raw PPG signal. While the provided label is not from only reading the raw PPG signal but taking other channels into account, we would like to bring to readers' attention that the meaning of the signal quality might be reconsidered.

To dig deeper, we find that the PPG segment encompasses not only the cardiac component (shown in the fourth row) but also a strong motion rhythm (shown in the third row), where we apply SAMD [1] to get these components. The quality of the decomposition can be visualized by the summation of the decomposed cardiac component and motion rhythm that is superimposed as the red curve on the second row. The normalized root mean squared error (NRMSE) is 0.235. We may consider the decomposed cardiac component of high quality (black curve in the fourth row, with R peaks from the ECG shown as vertical gray lines for comparison).

The time-frequency representation (TFR) of the PPG segment determined by SST shown in the left panel of Figure 2 provides additional insights. Examining multiple curves with a non-integer multiple relationship suggests the presence of multiple oscillatory components. Specifically, two nearly parallel lines appear at approximately 2 and 2.6 Hz, associated with the fundamental frequency of the cardiac component (heart rate) and the second harmonic of the motion rhythm, respectively. In other words, the motion rhythm is at about 1.3Hz, but its fundamental component is weak, or even missing, in the PPG signal and we only see the second, third and fourth harmonics indicated by blue arrows. See the right panel of Figure 2 for the TFR of the motion rhythm, which comes from subtracting the cardiac component from the PPG signal, where the pink dashed box indicates the region around 1.3Hz. Also see Figure 3 for a concrete evidence that the motion rhythm is about 1.3Hz, where the TFRs of the simultaneously recorded Inertial measurement unit (IMU) signal analyzed from different aspects are shown. It is important to note that the TFRs vary based on the perspective from which the IMU signal, as a vector-valued function, is analyzed. In the TFR of the magnitude of the IMU signal, curves are visible at 2.6 and 5.2 Hz, but not at 1.3 Hz. However, in the TFR of each axis, a curve appears at 1.3 Hz. This disparity arises from different WSFs associated with how we analyze the IMU signal as a multivariate time series. It is also worth noting that the motion rhythm depends on both the running speed and stride length. On the other hand, the HR gradually increases from 1.99 Hz to 2.11 Hz, while the motion rhythm keeps constant. As a result, the frequencies of the second harmonic of the cardiac component and the third

harmonic of motion rhythm depart as time proceeds, which leads to the spectral interference in the first half of the signal indicated by the pink dashed box in the left panel of Figure 2. After removing the cardiac component, we can see three obvious lines indicated by blue arrows in the right panel of Figure 2, which are associated with the second, third and fourth harmonics of the motion rhythm. This fact is reflected in the decomposed motion rhythm shown in the third row of Figure 1, where we can see a repeating pattern indicated by the blue box, which seems to have two cycles, but these two cycles are actually one thanks to the third harmonic. In this TFR, only two dominant harmonics of the cardiac component indicated by pink arrows are visible, likely due to the application of a strong low-pass filter with a cutoff frequency of 5 Hz to the database. This partially explains why the decomposed cardiac component differs from the typical PPG signal recorded during rest. Overall, through SAMD and TFR, we gain insight into the construction of the seemingly chaotic PPG signal, prompting a reconsideration of signal quality.

In another illustration (Figure 4) also from the TROIKA database [23], we present a PPG segment labeled "no-artifact" (or high quality, shown as the gray curve in the top row). This segment is the 65.5th second to the 76th second segment from the recordings of the 12th subject in the TROIKA database (`DATA_12_TYPE02.mat`), and the subject is also running at the speed of 6 kilometer per hour in this segment. The label seems reasonable since the PPG segment mimics cardiac oscillations. However, these cycles do not align with true cardiac rhythm, which is confirmed by reading the simultaneously recorded ECG signal (red curve in the fourth row), where again the R peak locations are superimposed on the second row as gray vertical lines. This segment includes multiple oscillatory components, including the cardiac component (fourth row, with ECG in red) and the motion rhythm (third row, with accelerometer magnitude in red), which is guided by the TFR shown in the left panel of Figure 5. Notably, the decomposed cardiac component reveals an oscillation pattern distinct from the raw signal, aligning well with the confirmed cardiac rhythm from the simultaneously recorded ECG. If our scientific interest lies in the motion rhythm or the cardiac component, the quality of this PPG should be considered high. While the experts' label appears to align with this observation, it stems from a different perspective. It is worth mentioning that unlike the signal shown in Figure 1, the motion rhythm in this segment has a clear fundamental component, which is represented as a line at 1.3 Hz shown in both TFRs of Figure 5 indicated by a blue arrow in the green dashed box (also see Figure 6 for the TFRs of the simultaneously recorded IMU signal). This fundamental component results in the up-down pattern of the troughs in the reconstructed motion rhythm depicted in the third row in Figure 4, particularly by the blue dashed box.

Based on the two examples above (and more shown in the supplementary material), we advocate a reconsideration of what constitutes "high quality" when analyzing PPG signals. Consider Figures 1 and 4 again. Both PPG signals not only exhibit a clear cardiac component (in the fourth row) but also a distinct motion rhythm, displaying different patterns. Therefore, if the scientific focus is on cardiac dynamics, depending on the targeting problem, the signal should be deemed of high quality, though this fact is not evident from the raw PPG signal, even if other channels are considered to help the annotation. Similarly, if the goal is to study the motion rhythm, this PPG should *also* be considered "high quality" since it contains a component oscillating at the same frequency as the simultaneously

recorded accelerometer magnitude signal. Once again, however, this fact is not apparent from the raw PPG signal alone.

Our conclusion is that relying on the raw PPG signal for signal quality assessment may introduce bias, even when it is a human expert that labels the quality and other channels are used. An alternative and systematic approach based on signal decomposition for determining signal quality is warranted and it will be our future direction.

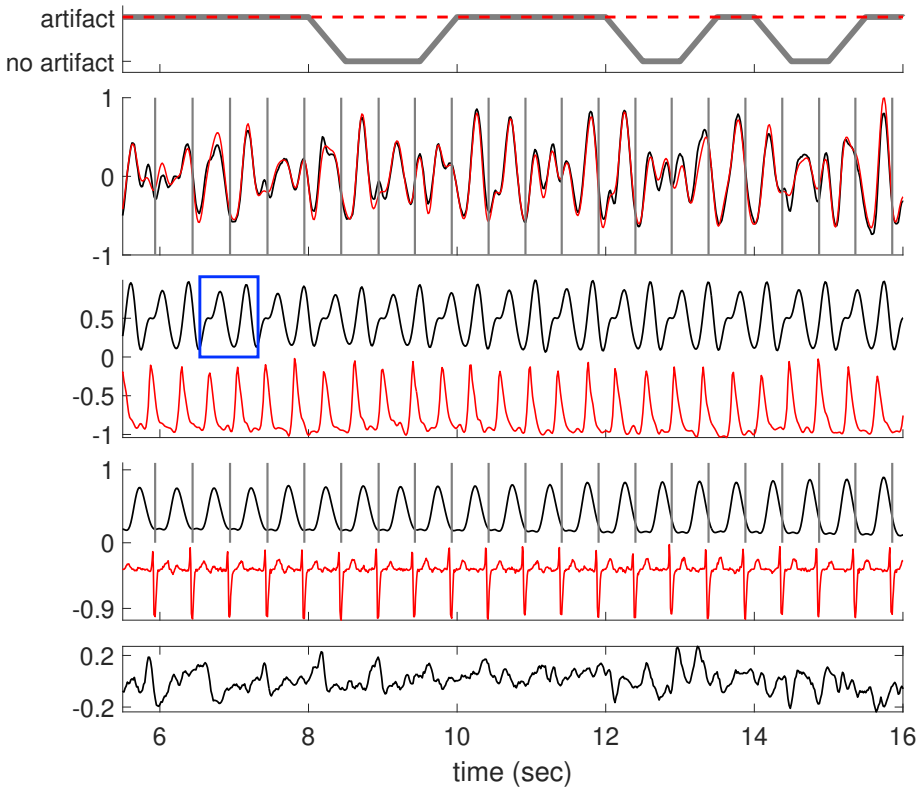

FIGURE 1. The 65.5th to the 76th second segment of the 6th subject in the TROIKA datasets, who is running at the speed of 6 kilometer per hour during this segment. **The 1st row:** Label sequence (grey line) and the prediction result by the proposed SQA model (red-dashed line). **The 2nd row:** The raw PPG signal is shown in black, and the summation of the decomposed motion rhythm and cardiac component is superimposed in red. **The 3rd row:** The decomposed motion rhythm (black curve) and the synchronously recorded accelerometer magnitude signal (red curve). **The 4th row:** The decomposed cardiac component (black curve), the synchronously recorded ECG (red curve) and the detected R-peaks (grey lines). **The 5th row:** The difference of the raw PPG signal and the summation of the decomposed motion rhythm and cardiac component. The decomposition NRMSE is 0.235.

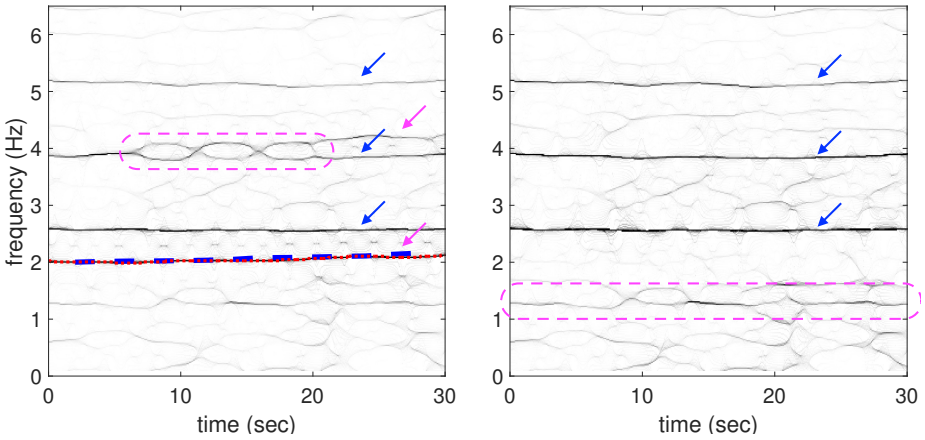

FIGURE 2. The TFR of the 60th to the 90th second PPG segment of the 6th subject in the TROIKA datasets, who is running at the speed of 6 kilometer per hour during this segment. We show the second-order SST with the Gaussian window with $\sigma = 1.5$ second. **Left:** The TFR of the original PPG signal, where the blue-dashed line is the ECG-derived IHR, and the red-dotted line is the result of the RD algorithm. **Right:** The TFR of the PPG signal after removing the cardiac component.

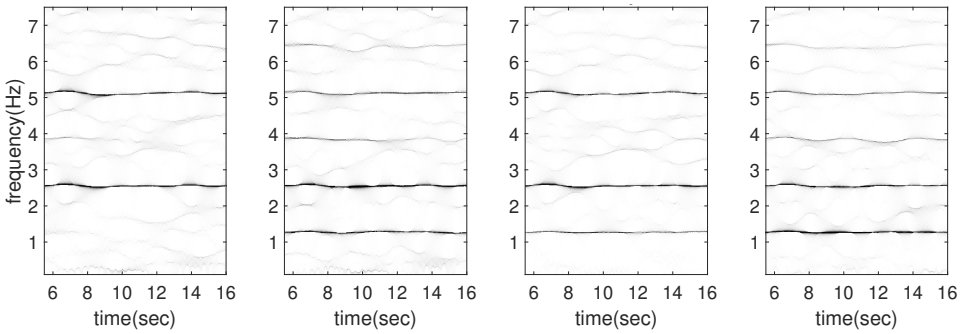

FIGURE 3. The TFR of the 60th to the 90th second IMU segment of the 6th subject in the TROIKA datasets, who is running at the speed of 6 kilometer per hour during this segment. We show the second-order SST with the Gaussian window with $\sigma = 1.5$ second. From left to right: the TFR of the magnitude of the IMU signal, and the acceleration along the x-axis, y-axis and z-axis.

4. CONCLUSION

The main contribution is showing the necessity of reconsidering the meaning of high quality PPG signals by providing evidence based on the ANHM for the PPG signal and a signal decomposition algorithm. The same consideration can be extended to other biomedical signals that we do not explore in this paper. In conclusion, the exploration presented in this paper underscores the necessity for designing a new signal quality evaluation system, especially when dealing with PPG signals recorded in the free-living environment. Our proposed ANHM model, in

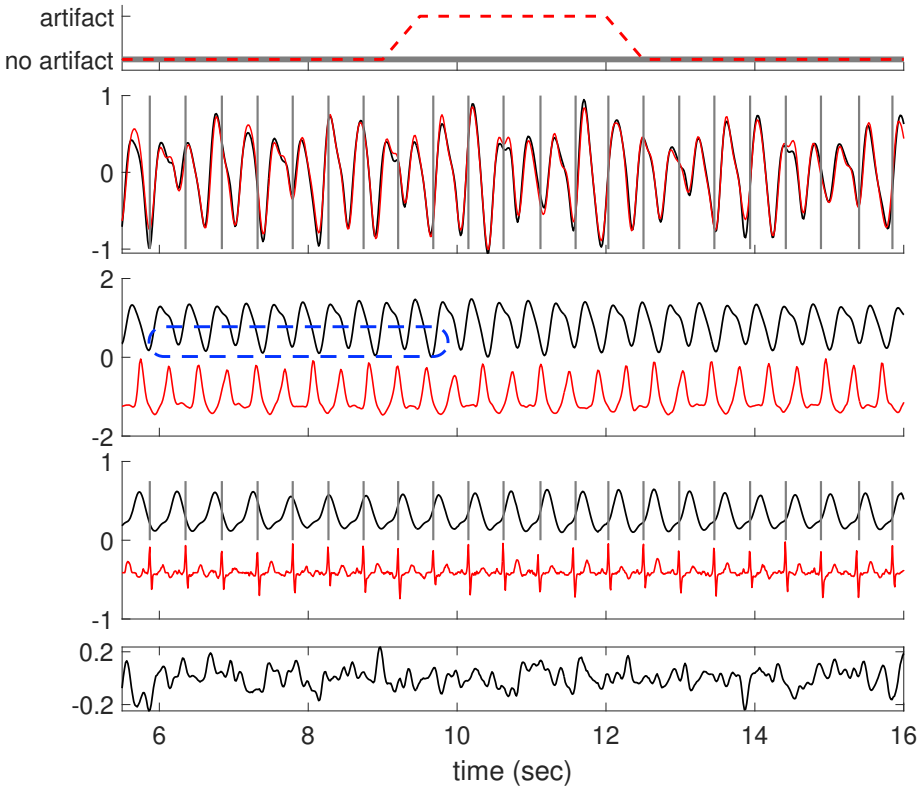

FIGURE 4. The 65.5th to 76th second segment of the 12th subject in the TROIKA datasets, who is running at the speed of 6 kilometer per hour during this segment. **The 1st row:** Label sequence (grey line) and the prediction result by the proposed SQA model (red-dashed line). **The 2nd row:** The raw PPG signal is shown in black, and the summation of the decomposed motion rhythm and cardiac component is superimposed in red. **The 3rd row:** The decomposed motion component (black curve) and the synchronously recorded accelerometer magnitude signal (red curve). **The 4th row:** The decomposed cardiac component (black curve), the synchronously recorded ECG (red curve) and the detected R-peaks (grey lines). **The 5th row:** The difference of the raw PPG signal and the summation of the decomposed motion rhythm and cardiac component. The decomposition NRMSE is 0.194.

conjunction with advanced signal decomposition tools, holds promise for establishing such a system by incorporating the signal decomposition step. The development of this system will be reported in our future work. With labels provided by this system, we believe we can advance towards establishing a more dependable SQA model, particularly for scientific research.

ACKNOWLEDGEMENT

The authors express gratitude to the authors in [6] for their assistance in providing details regarding the labeled databases they shared.

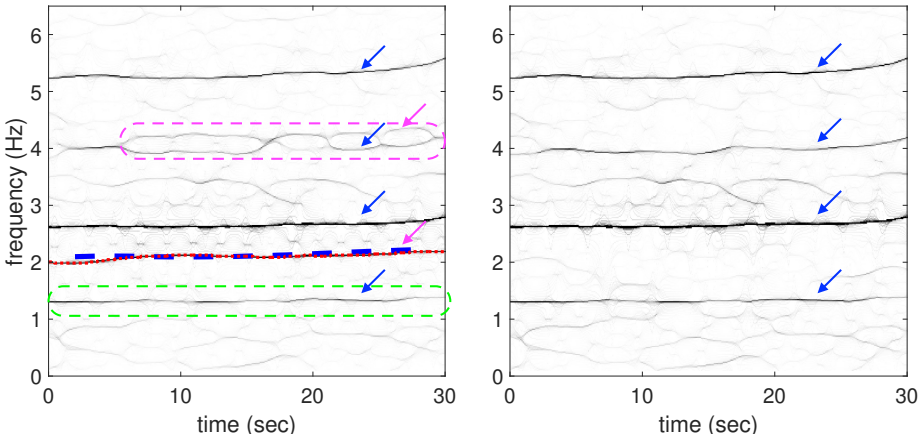

FIGURE 5. The TFR of the 60th to the 90th second PPG segment of the 12th subject in the TROIKA datasets, who is running at the speed of 6 kilometer per hour during this segment. We show the second-order SST with the Gaussian window with $\sigma = 1.5$ second. **Left:** The TFR of the original PPG signal, where the blue-dashed line is the ECG-derived IHR, and the red-dotted line is the result of the RD algorithm. **Right:** The TFR of the PPG signal after removing the cardiac component.

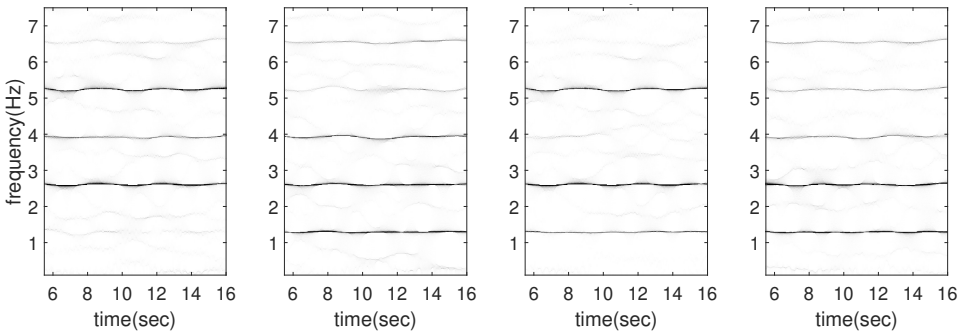

FIGURE 6. The TFR of the 60th to the 90th second IMU segment of the 12th subject in the TROIKA datasets, who is running at the speed of 6 kilometer per hour during this segment. We show the second-order SST with the Gaussian window with $\sigma = 1.5$ second. From left to right: the TFR of the magnitude of the IMU signal, and the acceleration along the x-axis, y-axis and z-axis.

REFERENCES

[1] Marcelo A Colominas and Hau-Tieng Wu. Decomposing non-stationary signals with time-varying wave-shape functions. *IEEE Trans. Signal Process*, 69:5094–5104, 2021.

[2] Ingrid Daubechies, Jianfeng Lu, and Hau-Tieng Wu. Synchrosqueezed wavelet transforms: an empirical mode decomposition-like tool. *Appl. Comput. Harmon. Anal.*, 30(2):243–261, 2011.

[3] Nathalie Delprat, Bernard Escudié, Philippe Guillemain, Richard Kronland-Martinet, Philippe Tchamitchian, and Bruno Torresani. Asymptotic wavelet and gabor analysis: Extraction of instantaneous frequencies. *IEEE Trans. Inf. Theory*, 38(2):644–664, 1992.

[4] Mohamed Elgendi. Optimal signal quality index for photoplethysmogram signals. *Bioengineering*, 3, 2016.

[5] P. Flandrin. *Time-frequency/time-scale analysis*, volume 10. Academic Press Inc., San Diego, 1999.

[6] Zhicheng Guo, Cheng Ding, Xiao Hu, and Cynthia Rudin. A supervised machine learning semantic segmentation approach for detecting artifacts in plethysmography signals from wearables. *Physiological Measurement*, 42(12):125003, dec 2021.

[7] B.S. Kim and S.K. Yoo. Motion artifact reduction in photoplethysmography using independent component analysis. *IEEE Transactions on Biomedical Engineering*, 53(3):566–568, 2006.

[8] Panicos A Kyriacou and John Allen. *Photoplethysmography: Technology, Signal Analysis and Applications*. Academic Press, 2021.

[9] Han-Wook Lee, Ju-Won Lee, Won-Geun Jung, and Gun-Ki Lee. The periodic moving average filter for removing motion artifacts from ppg signals. *International Journal of Control, Automation and Systems*, 5, 12 2007.

[10] Chen-Yun Lin, Li Su, and Hau-Tieng Wu. Wave-shape function analysis–when cepstrum meets time-frequency analysis. *J. Fourier Anal. Appl.*, 24(2):451–505, 2018.

[11] Elisa Mejia-Mejia, John Allen, Karthik Budidha, Chadi El-Hajj, Panicos A. Kyriacou, and Peter H. Charlton. 4 - photoplethysmography signal processing and synthesis. In John Allen and Panicos Kyriacou, editors, *Photoplethysmography*, pages 69–146. Academic Press, 2022.

[12] Serena Moscato, Stella Lo Giudice, Giulia Massaro, and Lorenzo Chiari. Wrist photoplethysmography signal quality assessment for reliable heart rate estimate and morphological analysis. *Sensors*, 22(15), 2022.

[13] Patrick Mullan, Christoph M. Kanzler, Benedikt Lorch, Lea Schroeder, Ludwig Winkler, Larissa Laich, Frederik Riedel, Robert Richer, Christoph Luckner, Heike Leutheuser, Bjoern M. Eskofier, and Cristian Pasluosta. Unobtrusive heart rate estimation during physical exercise using photoplethysmographic and acceleration data. In *2015 37th Annual International Conference of the IEEE Engineering in Medicine and Biology Society (EMBC)*, pages 6114–6117, 2015.

[14] Emad Kasaeyan Naeini, Iman Azimi, Amir M. Rahmani, Pasi Liljeberg, and Nikil Dutt. A real-time ppg quality assessment approach for healthcare internet-of-things. *Procedia Computer Science*, 151:551–558, 2019. The 10th International Conference on Ambient Systems, Networks and Technologies (ANT 2019) / The 2nd International Conference on Emerging Data and Industry 4.0 (EDI40 2019) / Affiliated Workshops.

[15] Thomas Oberlin, Sylvain Meignen, and Valérie Perrier. Second-order synchrosqueezing transform or invertible reassignment? towards ideal time-frequency representations. *IEEE Trans. Signal Process*, 63(5):1335–1344, 2015.

[16] Christina Orphanidou. *Signal Quality Assessment in Physiological Monitoring: State of the Art and Practical Considerations*. 01 2018.

[17] Fulai Peng, Hongyun Liu, and Weidong Wang. A comb filter based signal processing method to effectively reduce motion artifacts from photoplethysmographic signals. *Physiological Measurement*, 36(10):2159, sep 2015.

[18] S. M. A. Salehizadeh, Duy K. Dao, Jo Woon Chong, David McManus, Chad Darling, Yitzhak Mendelson, and Ki H. Chon. Photoplethysmograph signal reconstruction based on a novel motion artifact detection-reduction approach. part ii: Motion and noise artifact removal. *Annals of Biomedical Engineering*, 42(11):2251–2263, Nov 2014.

[19] Kirk H Shelley. Photoplethysmography: beyond the calculation of arterial oxygen saturation and heart rate. *Anesthesia & Analgesia*, 105(6):S31–S36, 2007.

[20] Yan-Wei Su, Gi-Ren Liu, Yuan-Chung Sheu, and Hau-Tieng Wu. Ridge detection for nonstationary multicomponent signals with time-varying wave-shape functions and its applications. *arXiv preprint arXiv:2309.06673*, 2023.

[21] J Abdul Sukor, S J Redmond, and N H Lovell. Signal quality measures for pulse oximetry through waveform morphology analysis. *Physiological Measurement*, 32(3):369, feb 2011.

[22] H.-T. Wu. Instantaneous frequency and wave shape functions (I). *Appl. Comput. Harmon. Anal.*, 35:181–199, 2013.

[23] Zhilin Zhang, Zhouyue Pi, and Benyuan Liu. Troika: A general framework for heart rate monitoring using wrist-type photoplethysmographic signals during intensive physical exercise. *IEEE Transactions on Biomedical Engineering*, 62(2):522–531, 2015.

Department of Applied Mathematics, National Yang Ming Chiao Tung University, Hsinchu, Taiwan
E-mail address: su311652001.sc11@nycu.edu.tw

Department of Mathematics, National Taiwan University, Taipei, Taiwan
E-mail address: allenh18.ee08@nycu.edu.tw

Department of Mathematics, National Chen-Kung University, Tainan, Taiwan and National Center for Theoretical Sciences, National Taiwan University, Taipei, Taiwan
E-mail address: girenliu@gmail.com

Department of Applied Mathematics, National Yang Ming Chiao Tung University, Hsinchu, Taiwan
E-mail address: sheu@math.nctu.edu.tw

Courant Institute of Mathematical Sciences, New York University, New York, NY, 10012 USA
E-mail address: hauwu@cims.nyu.edu